TRITA-A
Report
ISSN 1102-2051
ISRN KTH/ALF/--01/2--SE

KTH-ALF--01-2

KTH

Reactor Potential for Magnetized Target Fusion

Jon-Erik Dahlin

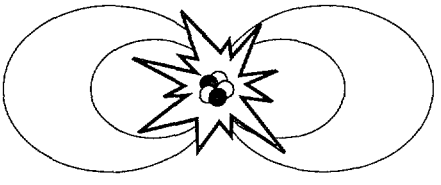

Research and Training programme on
CONTROLLED THERMONUCLEAR FUSION
AND PLASMA PHYSICS
(Association EURATOM/NFR)

FUSION PLASMA PHYSICS
ALFV N LABORATORY
ROYAL INSTITUTE OF TECHNOLOGY
SE-100 44 STOCKHOLM SWEDEN

PLEASE BE AWARE THAT
ALL OF THE MISSING PAGES IN THIS DOCUMENT
WERE ORIGINALLY BLANK

TRITA-ALF-2001-02
ISRN KTH/ALF/--01/2--SE

Reactor Potential for Magnetized Target Fusion

J.-E. Dahlin

Stockholm, June 2001

The Alfvén Laboratory
Division of Fusion Plasma Physics
Royal Institute of Technology
SE-100 44 Stockholm, Sweden
(Association EURATOM/NFR)

Printed by
Alfvén Laboratory
Fusion Plasma Physics Division
Royal Institute of Technology
SE-100 44 Stockholm

Abstract

Magnetized Target Fusion (MTF) is a possible pathway to thermonuclear fusion different from both magnetic fusion and inertial confinement fusion. An imploding cylindrical metal liner compresses a preheated and magnetized plasma configuration until thermonuclear conditions are achieved.

In this report the Magnetized Target Fusion concept is evaluated and a zero-dimensional computer model of the plasma, liner and circuit as a connected system is designed. The results of running this code are that thermonuclear conditions are achieved indeed, but only during a very short time.

At peak compression the pressure from the compressed plasma and magnetic field is so large reversing the liner implosion into an explosion. The time period of liner motion reversal is termed the dwell time and is crucial to the performance of the fusion system. Parameters as liner thickness and plasma density are certainly of significant importance to the dwell time, but it seems like a reactor based on the MTF principle hardly can become economic if not innovative solutions are introduced. In the report two such solutions are presented as well.

Contents

List of Figures

Chapter 1

Introduction

1.1 Why do we need fusion power?

The total energy consumption worldwide is over 10 TW and rising. The main part of this energy is produced by consumption of fossil fuels such as coal, oil and fossil gas. Probably the oil wells will start to dry some time in the middle of the present century and coal production is expected to start to decrease some time within the next hundred years or so. The prices of petroleum products and fuels will unavoidably rise. If there are no alternative energy sources by then, capable of replacing fossil fuels as the foundation of energy production in society, the world will undoubtedly be exposed to massive economic crises.

Today it is accepted in most parts of the scientific society that the combustion of fossil fuels will cause global climate changes, and that this will certainly happen within a time scale shorter than the lifetime of these fuels based upon their availability. Connected to these changes, which may be severe already early in this century, are changes in the ecosystems. This will put demands on agriculture and may decrease crops, which would result in large amounts of refugees. Again we face an economic problem with huge dimensions.

The problem with energy production based on consumption of fossil fuels is hence twofold: the fuel availability will eventually decrease and the combustion of coal leads likely to severe climate changes. Both problems will lead to economic stress on society and it is thus enormously important to alter the focus from fossil fuels to alternative energy sources.

Today there are no alternatives that could take over completely. Hydropower is relatively environmentally friendly, it is a renewable energy source and has the capability of large-scale energy production but is difficult or even impossible to expand to the scale of fossil fuel energy production. Nuclear power is also relatively environmentally friendly and is indeed possible to expand. The problem with nuclear power is however the limited

availability of fuels. Renewable energy sources such as wind power, solar power and energy crops face the problems of large areal demands and large investment costs.

Fusion power could certainly be the solution. It is not a renewable energy source, but the availability of the fuels is almost unlimited since deuterium can be extracted from seawater to low costs. If tritium is used it has to be produced within the reactor but not even this would be a large problem. It should however be noted that fusion power is not free from drawbacks. Its disadvantages include the radioactive loading of wall material (which has to been taken care of, even though the amounts of radioactive trashes are far less then from conventional nuclear power plants, and the trashes are also far less active), the risks connected to handling radioactive fuel (if tritium is used) and the quite large costs for developing the technology and construction of facilities, which will effect the cost of energy.

1.2 Magnetized Target Fusion

To this day, two main roads have been traveled to find a working fusion concept. In the Magnetic Fusion Energy (MFE) branch, a plasma containing fusion fuels (most often deuterium and tritium) is confined by a strong magnetic field and heated to thermonuclear conditions. The configuration that has been most examined is the Tokamak, a toroidal (i.e. doughnut shaped) configuration with a strong toroidal magnetic field. In the Tokamak the coils producing this field must be superconducting which implies the device to be very expensive. The International Tokamak Experimental Reactor (ITER), which is expected to achieve ignition conditions, i.e. no external heating of the plasma is needed but the fusion reactions are sufficient to heat the plasma to sustain thermonuclear fusion conditions, is estimated to cost some \$5-10 billion. Other more economic configurations are examined as well, but so far plasma instabilities makes it unclear whether these could ever be developed into working reactors.

The other branch is the Inertial Confinement Fusion (ICF) branch. This concept is pulsed in nature and here a target pellet made from fusion fuels is compressed to thermonuclear conditions by an imploding spherical shell, and then confined during the pulse by its own inertia. Very powerful lasers or particle beams vaporizing the outer layer of the shell drive the implosion. When the outer layer is vaporized, the reaction force presses the shell inwards compressing the fuel. Also this concept is very expensive since the laser or beam drivers are extremely costly. The United States' National Ignition Facility (NIF) is planned to demonstrate ignition through ICF. The cost to build this facility will be around \$1 billion. It is clear that a cheaper and faster way to fusion would be greatly desirable.

Magnetic Fusion Energy works typically at fuel number densities of $n =$

10^{20} m^{-3} and temperature T = 10-40 keV (where the temperature notation so common in plasma physics is used where temperature is given in units of k_BT/e, thus T = 1 eV (11600 K). In Inertial Confinement Fusion the number density at peak compression is far larger: $n = 10^{31}$ m^{-3} is aimed at after a radial compression of a factor 30-40. It has been found that adding a magnetic field to the target drastically reduces the demands on the drivers due to magnetic insulation. A new regime in parameter space opens up between MFE and ICF with typical number density of $n = 10^{26}$ m^{-3} and temperature T = 10 keV. This density is significantly larger than MFE, which is interesting since reactivity scales as density squared, and system size can be reduced as all characteristic plasma-lengths decrease with density.

Magnetized Target Fusion (MTF) is the concept where a preheated *magnetized target* is compressed to thermonuclear conditions. The regime at aim is the one described above. However, the compression is not obtained through lasers or beams but an imploding solid metal liner driven by magnetic forces. The technology of imploding metal liners has been developed by the US Department of Energy (DOE) in purpose to understand megabar hydrodynamics but is relevant to MTF as well.

Several configurations have been examined whether to prove suitable for MTF, both spherical and linear ones. The plasma configuration at choice must be stable during the compression so that the fuel does not cool before burning. Problems are how to breakdown the gas and preheat the plasma avoiding too much impurities to be inserted, and indeed how to insert the fuel gas into a spherical liner configuration. A class of plasma configurations that seem to be stable enough is the compact toroid (CT) class, which in contrast to other toroidal configurations such as Tokamaks and Reversed Field Pinches (RFPs) has a small major radius and hence cannot be placed into a toroidal vacuum vessel. CTs have been studied during 20 years. They can be formed inside of, or translated into a cylindrical metal liner, and thereafter compressed as the liner implodes radially. The preheated CT-plasma should have a number density of around $n = 10^{23}$ and a temperature of T = 100-500 eV. It is then compressed with a radial convergence of 10 and thus heated by a factor of 100-1000 by the PdV work performed by the liner.

Another MTF solution is the staged Z pinch, which has been examined at the University of California in Irvine. In this concept the target plasma is a dense Z pinch plasma, formed by a cryogenic DT-fiber. The liner is a plasma annular to the target plasma, imploding due to self-pinching forces. As the axial magnetic field thus is compressed, the target plasma is heated adiabatically. This concept is however not further investigated within this report.

1.3 The pathway to a working fusion reactor

Los Alamos National Laboratory (LANL) in New Mexico, USA, has proposed a national interinstitutional Proof-of-Principle program to explore the MTF path to fusion. Their proposition is a three-year plan for $20 million to do liner on plasma experiments with existing facilities to examine the performance of the concept. If proving successful, LANL claims ignition could be achieved at the recently finished Atlas driver facility that has been built for other application at a cost of $50 million. If MTF holds its promises it can indeed become a fast, low cost pathway to a working fusion reactor.

1.4 Assumptions and notations used in this report

This report concerns the MTF concept and a zero-dimensional model of the plasma, liner and circuit as a connected system. The plasma compressed by the liner is thought to be homogenous and fill up the entire liner volume (which is cylindrical). The liner is made from aluminum. Magnetohydrodynamic conditions are assumed to be relevant for the plasma.

Quantities used are most often SI units but for temperature, as mentioned in section C.12, the notation $T = k_B T_K/e$ is used, where T_K is temperature given in Kelvin, e is the unit charge and k_B is Boltzmann's constant.

Chapter 2

Zero-dimensional model

2.1 Model conditions

2.1.1 Performance of the plasma

Within this work, the one plasma configuration that has been chosen as the most promising to be placed inside an imploding liner is the Field Reversed Configuration (FRC). The FRC is an elongated compact toroid without toroidal field. It can be formed by a theta pinch, successfully translated and trapped by mirror coils. The translation can be performed either by translation coils or by the formation theta coil if this is a conical theta coil. The FRC has showed to be stable both under static conditions and translation during several microseconds, which is the time scale relevant for liner implosions.

In the zero-dimensional model it is assumed that the target plasma is equally distributed over the cylindrical volume inside the liner at all time. A more rigorous analysis would consider the pressure and temperature gradients characterizing the field reversed plasma configuration.

Because of field-line tension, an FRC contracts along the symmetry axis as well as radially. Thus, although the volume is imploded only in two dimensions, the FRC is imploded somewhat in the third dimension as well. In the case of pure 2D-implosion of the liner (the liner is assumed to remain cylindrical throughout the whole implosion) the FRC implosion can be described as 2.4-dimensional, i.e. the volume of the configuration is proportional to the radius to the power of 2.4. Full 3D-implosion of the FRC can be accomplished if the liner is converging more in the ends. Such a liner convergence is obtained if the liner is made thinner (and therefore lighter) in the ends. If the implosion is 3D, requirements to the linear convergence and/or initial plasma parameters can be reduced. This means that the assumption that the plasma is equally distributed in the volume throughout the implosion, and thus only compressed in two dimensions, may be somewhat pessimistic.

Further, the plasma is assumed to contain only fusion fuel (equal amounts

of deuterium and tritium) and reaction ashes in the form of helium but no impurities. Of course this is an optimistic simplification, but the theta pinch formation of the FRC results in quite small amounts of impurities since no gap electrodes are in use. Also, the wall is a source of impurities and indeed the plasma is wall contained, i.e. it leans directly to the wall. However, the strong magnetic field introduced by external coils is not for containment but for insulation and the FRC has a separatrix that acts as a divertor separating the burning plasma from the wall plasma. Thus a thin wall sheet is formed between the liner wall and the separatrix. This suggests that the assumption that the plasma contains no impurities may not be that bad after all as a first approximation.

2.1.2 Performance of the liner

The liner is an aluminum cylinder press fit between two electrodes. When a voltage is applied over the electrodes, a current flows axially through the liner. Self-pinching magnetic forces compresses the aluminum cylinder with velocities of the moving wall of up to 10-20 km/s. The kinetic energy of the imploding liner exceeds its vaporization energy, why this high implosion velocity is termed hypervelocity.

The choice of liner material is not an obvious one. At present day experiments with imploding liners made of aluminum have been done, mainly to investigate properties of high-pressure hydrodynamics, so most experience in imploding liners come from aluminum liners. Which liner material that will fit best the demands of MTF is still an open question.

During implosion, the liner material is assumed to be incompressible. This forces the thickness of the liner to increase as the liner radius decreases. The thickness as a function of liner radius $d(R)$ can be expressed as:

$$d(R) = -R + \sqrt{R^2 + d_0^2 + 2R_0 d_0} \tag{2.1}$$

where d_0 is the initial liner thickness and R_0 is the initial liner radius. For detailed investigations liner compressibility should be taken into account as it acts as a source for energy losses. However, treating the liner as incompressible still works very well as a good approximation.

The current flowing through the liner will, due to liner resistivity, heat the liner. A detailed study must take this heating and the following change in resistivity into account. For the purposes of this work it should however be enough to consider the resistivity to be constant. In fact, the resistance of the liner is much smaller than the resistance of the whole circuit, why the liner resistance here is totally ignored. Yet, the heating of the liner is important to be evaluated. At some point it will melt the liner, or even vaporize it. Since the time scale is so short, no cooling is considered and the only important quantity to consider is the total electric energy input into

the liner. This quantity in turn is proportional to the integral of the surface current of the cross section of the liner squared:

$$I_a = \int_t \frac{I(t)^2}{A_0^2} dt \tag{2.2}$$

The integral I_a is called the *action integral*. The parameter A_0 is the initial area of the liner cross section (which due to incompressibility of the liner material in this model is constant) and $I(t)$ is the total liner current at time t. If the integral is below about $2{\cdot}10^{16}$ A^2s/m^4, at least part of the liner will be solid. If it is below about $4{\cdot}10^{16}$ A^2s/m^4, at least part of the liner will be liquid and if it exceeds about $5{\cdot}10^{16}$ A^2s/m^4, it will be totally melted and part of the liner will probably be vaporized [I.R. Lindemuth, personal communication]. It is probably important to choose system parameters so that the liner is not melted and vaporized. However, one should be careful in these matters. After all, the technology is just being developed. Maybe a liquid liner will show to be a preferred solution.

2.1.3 The circuit

A realistic model should consider not only the plasma and the liner but also the electrical circuit. All these three model units interact on one another and their behaviour influence the behaviour of all the others.

Energy is stored in a capacitor bank, which is connected to the liner in series. A schematic picture of the circuit can be seen in figure 2.1.3. The liner is treated as a variable inductor and the liner resistance is ignored.

The feed system is coaxial to the liner so that the return current from the cathode is closing the circuit via a path outside the liner. This implies the total inductance of the system to be:

$$L_{tot} = \frac{\mu_0 l}{2\pi} \cdot ln\frac{a}{R} + \frac{\mu_0 l}{8\pi} \tag{2.3}$$

which can be divided into L_{out} and L_l as:

$$L_{out} = \frac{\mu_0 l}{8\pi} \tag{2.4}$$

$$L_l = \frac{\mu_0 l}{2\pi} \cdot ln\frac{a}{R} \tag{2.5}$$

where μ_0 is the permeability in empty space, l is the length of the liner, R is the radius of the liner (which of course is varying) and a is the distance from the liner symmetry axis to the return current path.

2.1.4 Alpha particle deposition

In a fusion reactor, alpha particles produced in the nuclear reactions are expected to heat the plasma. The steady state reactor aims at ignition, which occurs when the heating from alpha particles equals the energy losses, and thus no additional heating is needed. In the MTF concept alpha particle heating may contribute to the energy input depending on the axial magnetic field and the burn time.

In a typical MTF device, an initial axial magnetic field of 5 T is introduced to a plasma with radius 5 cm. At peak compression the radius is 0.5 cm and therefore the B_Z-field is $B_Z = 500$ T. Alpha particles produced by merging deuterium and tritium has a kinetic energy of $T_\alpha = 3.5$ MeV. The Larmor radius of the alpha particles is given by

$$\rho_a = \frac{\sqrt{2T_\alpha m_\alpha}}{2eB} \tag{2.6}$$

where m_α is the mass of a helium nucleus and e is the unit charge. This implies the Larmor radius to be 0.054 cm, or 10.8% of the liner radius at peak compression. If there is no transport of alpha particles orthogonal to the magnetic field on the time scale relevant for plasma burning (up to a few 100 ns), only those alphas that hit the wall within their gyration are lost. Since the Larmor radius is 10.8% of the liner radius, 43.2% of the alphas will be lost during their first gyration.

Accordingly, 56.8% of the alpha particles can take part in the plasma heating at most. However, since the plasma is only burning as long as the volume is compressed, only alpha particles that manage to leave their kinetic energy to the fusion fuel within the burn time take part in the heating.

The deceleration of fast alpha particles does not heat the ions directly, but heat the electrons of the plasma, which in turn heat the ions. The reason for this is that the equipartition time for ions and electrons is far shorter than the helium to deuterium or helium to tritium equipartition times. The equipartition time for electrons and fusion fuel ions is in the order of 1 μs, which is almost an order of magnitude greater than the burn time. For this reason, no alpha particle heating at all is considered in this model. However, if an MTF configuration is proposed that have a large burn time, alpha particle heating can of course come to play a significant role.

2.2 Equations of performance

As the liner compresses the plasma, it is heated thermally. In this zero-dimensional model, the following equations are used to describe the whole system of the plasma configuration, the liner and the electric circuit.

2.2.1 Force balance

Early in the implosion of the liner, the deformation becomes plastic and in this model no elastic forces from Hooks law are considered.

What is considered, is the magnetohydrodynamic (MHD) equation of motion:

$$\rho\frac{d\mathbf{v}}{dt} = \mathbf{j}\times\mathbf{B} - \nabla p \tag{2.7}$$

This equation describes the radial force balance of the liner. The magnetic field $\mathbf{B}$ inside the liner is a consequence of the axial liner current. It is defined as:

$$B_\theta(r) = \frac{\mu_0 I(r)}{2\pi r} \tag{2.8}$$

Only the θ-component of B is nonzero, and the B_Z-field inside the plasma does not penetrate the liner material. In equation (2.8) $I(r)$ is the total current inside r.

At steady state, the radial force balance is:

$$\mathbf{j}\times\mathbf{B} - \nabla p = 0 \tag{2.9}$$

Now Ampre's law is introduced:

$$\nabla\times\mathbf{B} - \mu_0\mathbf{j} \tag{2.10}$$

Insertion of equation (2.10) into equation (2.9) gives with some rearrangement and also using equation (2.8):

$$\mu_0 r^2\frac{dp}{dr} = -\frac{1}{2}\left(\frac{\mu_0}{2\pi}\right)^2\frac{d}{dr}I(r)^2 \tag{2.11}$$

If the liner thickness d is small, integrating the left-hand side of equation (2.11) over the liner gives:

$$\mu_0\int_R^{R+d} r^2\frac{dp}{dr}dr \approx \mu_0 R^2\int_{p(R)}^{p(R+d)} dp = \mu_0 R^2\left(p(R+d) - p(R)\right) \tag{2.12}$$

$$\Rightarrow \mu_0\int_R^{R+d} r^2\frac{dp}{dr}dr \approx \mu_0 R^2\left(0 - 2neT - \frac{B_Z^2}{2\mu_0}\right) \tag{2.13}$$

where R is the liner inner radius, $2neT$ is the plasma pressure at the liner inner surface and $B_Z^2/(2\mu_0)$ is the magnetic pressure from the axial magnetic field inside the plasma.

Integrating the right-hand side of equation (2.11) over the liner gives:

$$-\frac{1}{2}\left(\frac{\mu_0}{2\pi}\right)^2\int_R^{R+d}\frac{d}{dr}I(r)^2 dr = -\frac{1}{2}\left(\frac{\mu_0}{2\pi}\right)^2 I^2 \tag{2.14}$$

Thus, the radial balance at steady state is:

$$0 = -\frac{\mu_0 I^2}{8\pi^2 R^2} + 2neT + \frac{B_Z^2}{2\mu_0} \tag{2.15}$$

Now, the inertia-term integrated radially over the liner is given by:

$$\langle \rho \frac{d\mathbf{v}}{dt} \rangle_r \approx \rho \frac{d^2 R}{dt^2} \tag{2.16}$$

$$\int_R^{R+d} \rho \frac{d^2 R}{dt^2} dr \approx \rho \frac{d^2 R}{dt^2} \int_R^{R+d} dr = \rho d \frac{d^2 R}{dt^2} \tag{2.17}$$

Again, it is assumed that the liner is thin. Altogether, the radial equation of motion can now be written as:

$$\rho d \frac{d^2 R}{dt^2} = -\frac{\mu_0 I^2}{8\pi^2 R^2} + 2neT + \frac{B_Z^2}{2\mu_0} \tag{2.18}$$

2.2.2 Power balance

The thermal energy of the plasma must at all times equal the total energy input minus the energy losses. At each point of time the following equation must be satisfied:

$$3ne \frac{dT}{dt} = -p\nabla \cdot \mathbf{v} + P_\alpha - P_{rad} \tag{2.19}$$

As has already been stated is section 2.1.4, no alpha particle energy input is considered. Consequently P_α is zero.

In this zero-dimensional model the plasma has no inner structure whatsoever, and therefore n, T and p are constant within the plasma volume. Also the first term in the right-hand side of equation (2.19) should be radially averaged:

$$\langle p\nabla \cdot \mathbf{v} \rangle_r = \int_0^R \frac{2\pi r}{\pi R^2} (p\nabla \cdot \mathbf{v})\, dr \tag{2.20}$$

Assume that $\mathbf{v}$ is only varying radially:

$$\int_0^R \frac{2\pi r}{\pi R^2} (p\nabla \cdot \mathbf{v})\, dr = \frac{2p}{R^2} \int_0^R \frac{d}{dr} (r v_r)\, dr \tag{2.21}$$

Since $v_r(r) = dR/dt$ and the total plasma volume is $V = \pi R^2 l$, the expression (2.21) can be written as:

$$\frac{2p}{R^2} \int_0^R \frac{d}{dr} (r v_r)\, dr = \frac{p}{V} \frac{dV}{dt} \tag{2.22}$$

Thus the plasma power balance should be written:

$$3ne \frac{dT}{dt} = -\frac{p}{V} \frac{dV}{dt} + P_\alpha - P_{rad} \tag{2.23}$$

The volume derivative is $dV/dt = 2\pi l R \cdot dR/dt$, which modifies equation (2.23) to:

$$3ne \frac{dT}{dt} = -\frac{2p}{R} \frac{dR}{dt} + P_\alpha - P_{rad} \tag{2.24}$$

2.2.3 Density balance

The equations in the previous sections can be used to calculate the time dependence of the radius and the temperature, as well as quantities directly dependent on those, such as axial magnetic field $B_Z(R)$, liner thickness $d(R)$ and plasma volume $V(R)$. Number density and liner current as well as quantities depending on those are however not possible to calculate just using those equations. Since these quantities must be known to use the equations above, new equations to calculate them have to be formulated.

The hydrogen number density n_H, can quite easily be calculated for every point of time. It is of course depending on the volume, which is depending on the radius, but also on the reactivity which changes the absolute number of hydrogen nuclei within the plasma, N_H. Note that:

$$\frac{dn_H}{dt} = \frac{d}{dt}\left(\frac{N_H}{V}\right) = \frac{1}{V}\frac{dN_H}{dt} + N_H\frac{dV^{-1}}{dt} \tag{2.25}$$

where

$$\frac{1}{V}\frac{dN_H}{dt} = -n_D n_T \langle\sigma v\rangle_{DT} \tag{2.26}$$

and

$$N_H\frac{dV^{-1}}{dt} = -\frac{N_H}{V^2}\frac{dV}{dt} = -\frac{2n_H}{R}\frac{dR}{dt} \tag{2.27}$$

Accordingly, the hydrogen number density is given by:

$$\frac{dn_H}{dt} = -n_D n_T \langle\sigma v\rangle_{DT} - \frac{2n_H}{R}\frac{dR}{dt} \tag{2.28}$$

Here the reaction rate is used, which has the dimension of number of reactions per second and unit volume:

$$R_{DT} = n_D n_T \langle\sigma v\rangle_{DT} \tag{2.29}$$

It is dependent of only the hydrogen number density $n_H = 2n_D = 2n_T$ and the temperature T (as the reactivity $\langle\sigma v\rangle_{DT}$ is dependent of the temperature). In equation (2.40) the radiation effect P_{rad} as described in [5] is used

$$P_{rad} = 1.692 \cdot 10^{-38} n_e (n_H + 2n_{He})\sqrt{T} \tag{2.30}$$

which is dependent of n_H and T as well as the helium number density n_{He}, but this last quantity can easily be extracted from n_H if the initial number density n_0 and the initial plasma volume V_0 are given, i.e.:

$$n_{He} = \frac{1}{2}\left(n_0\frac{R_0^2}{R^2} - n_H\right) \tag{2.31}$$

When the total number density is asked for, it is given by:

$$n = n_H + n_{He} \tag{2.32}$$

under the condition that the plasma contains no impurities. For more details about the reactivity relation, see appendix A.

2.2.4 Circuit equation

Now only the liner current $I(t)$ is unknown. To calculate this quantity a model for the circuit must be introduced. In section 2.1.3 the circuit is described as it is considered to operate in the model. In that section the inductance was given as:

$$L_{tot} = \frac{\mu_0 l}{2\pi} \cdot ln\frac{a}{R} + \frac{\mu_0 l}{8\pi} \tag{2.33}$$

The total resistance R_c of the circuit and the capacitance C_C of the capacitor bank are taken as variable parameters.

Kirchhoff's voltage law is used:

$$u_C + u_L + u_R = 0 \tag{2.34}$$

The voltage over the inductor is given by:

$$u_L = \frac{d}{dt}(L_{tot}I) = L_{tot}\frac{dI}{dt} + I\frac{dL_{tot}}{dt} \tag{2.35}$$

The current is given by the voltage change over the capacitor as:

$$I(t) = C_C\frac{du_C}{dt} \tag{2.36}$$

This equation is together with Ohm's law for the resistance, $u_R = R_c I(t)$, inserted into equation (2.34). Also using equation (2.35) with the inductance expression (5.1) inserted, equation (2.34) becomes:

$$u_C + L_{tot}C_C\frac{d^2u_C}{dt^2} - C_C\frac{\mu_0 l}{2\pi R}\frac{dR}{dt}\frac{du_C}{dt} + R_c C_C\frac{du_C}{dt} = 0 \tag{2.37}$$

After some rearrangement this relation becomes:

$$\frac{d^2u_C}{dt^2} = \left(\frac{\mu_0 l}{2\pi L_{tot}R}\frac{dR}{dt} - \frac{R_c}{L_{tot}}\right)\frac{du_C}{dt} - \frac{1}{L_{tot}C_C}u_C \tag{2.38}$$

This relation together with equation (2.36) can be used to calculate the current for all times.

2.2.5 System of differential equations

At this point, a complete system of equations can be composed to model the liner, plasma and circuit. Equations used are:

$$\rho d\frac{d^2R}{dt^2} = -\frac{\mu_0 I^2}{8\pi^2 R^2} + 2neT + \frac{B_Z^2}{2\mu_0} \tag{2.39}$$

$$3ne\frac{dT}{dt} = -\frac{2p}{R}\frac{dR}{dt} + P_\alpha - P_{rad} \tag{2.40}$$

$$\frac{dn_H}{dt} = -n_D n_T \langle \sigma v \rangle_{DT} - \frac{2n_H}{R}\frac{dR}{dt} \tag{2.41}$$

$$\frac{d^2u_C}{dt^2} = \left(\frac{\mu_0 l}{2\pi L_{tot} R}\frac{dR}{dt} - \frac{R_c}{L_{tot}}\right)\frac{du_C}{dt} - \frac{1}{L_{tot}C_C}u_C \tag{2.42}$$

To solve this system of differential equations, some of the equations have to be split into two. Equation (2.39) and (2.42) are of second order, and these equations must be split so that their first derivative and second derivative can be treated separately. The relation $p = 2neT$ is also used. The new system of first order differential equations is then:

$$\frac{dR}{dt} = \dot{R} \tag{2.43}$$

$$\frac{d\dot{R}}{dt} = -\frac{\mu_0 I^2}{8\pi^2 \rho d R^2} + \frac{2neT}{\rho d} + \frac{B_Z^2}{2\mu_0 \rho d} \tag{2.44}$$

$$\frac{dT}{dt} = -\frac{4T}{3}\frac{\dot{R}}{R} + \frac{2P_\alpha}{3ne} - \frac{2P_{rad}}{3ne} \tag{2.45}$$

$$\frac{dn_H}{dt} = -n_D n_T \langle \sigma v \rangle_{DT} - 2n_H\frac{\dot{R}}{R} \tag{2.46}$$

$$\frac{du_C}{dt} = \dot{u_C} \tag{2.47}$$

$$\frac{d\dot{u_C}}{dt} = \left(\frac{\mu_0 l}{2\pi L_{tot}}\frac{\dot{R}}{R} - \frac{R_c}{L_{tot}}\right)\dot{u_C} - \frac{1}{L_{tot}C_C}u_C \tag{2.48}$$

In this form the system of differential equations is introduced to the computer in a MathCAD code. The computer code uses a fourth order Runge-Kutta differential equation solver to interpolate in time from a set of initial conditions. These initial conditions are chosen, as well as step size and number of steps, and are certainly parameters to be adjusted in order to optimize the performance of the system.

2.2.6 Fractional burnup

In the scope of energy production, the fusion energy produced in each pulse must exceed the energy input. Every fusion of one deuterium nucleus and one tritium nucleus results in $E_{fus} = 17.6$ MeV of energy, split upon one 14.1 MeV neutron and one 3.5 MeV helium nucleus (alpha particle). Hence the energy output of one pulse is proportional to the fractional burnup f_b, which is given by:

$$f_b = \frac{n_0 V_0 - N_H}{n_0 V_0} \tag{2.49}$$

This energy is transformed into electricity in a converter system with the efficiency η. The energy input is the energy stored in the capacitor bank.

This energy, the capacitor energy W_C, is dependent of the (initial) capacitor voltage u_{C0} and the capacitance C_C of the capacitor bank, and can be written:

$$W_C = \frac{1}{2} C_C u_{C0}^2 \tag{2.50}$$

There might be a possibility to recover some of the energy stored in the capacitor. This can be done if the current is not cut at peak compression but is used to recharge the capacitor during the second quarter period of the current cycle. More about this in section 5.1. This far, the liner is expected to loose contact with the electrodes after peak compression, and no energy is recovered.

The energy balance can be examined using the Q-value, i.e. the fusion energy over the energy input. The Q-value can be written:

$$Q = \frac{f_b n_0 V_0 E_{fus}}{C_C u_{C0}^2} \tag{2.51}$$

However, only electric energy can be reused to charge the capacitor bank for the next shot, and only electric energy can be distributed on the electric grid. Therefore, the interesting quantity is $Q_{el} = \eta Q$. Of course $Q_{el} > 1$ is imperative but to make a profitable fusion reactor Q_{el} should be several times greater then one.

2.3 Results

2.3.1 Fundamental results

When running the MathCAD code with the system of six differential equations as described in section 2.2.5, the following quantities are monitored as functions of time (or rather, as column vectors where each row corresponds to a certain point of time):

Quantity:	
Liner radius	$R(t)$
Liner velocity	$\dot{R}(t)$
Plasma temperature (in eV)	$T(t)$
Hydrogen number density	$n_H(t)$
Capacitor voltage	$u_C(t)$
Liner current	$I(t)$

In order to optimize the performance of the system (i.e. maximizing the relation between the fractional burnup and the total power input) system parameters can be varied. Parameters that can be altered are initial liner thickness, initial liner radius, liner length, initial axial magnetic field, initial plasma temperature, initial plasma density and circuit parameters as capacitance, total resistance, initial inductance and initial capacitor voltage.

The recently finished Atlas pulsed-power capacitor bank at the Los Alamos National Laboratory (LANL) may store 36 MJ of electric energy, and is enable to discharge in less than 10 μs. This should make it the most powerful capacitor bank in the world. It should be powerful enough to enable a preheated plasma configuration to be PdV-heated to at least near-thermonuclear conditions. In the table below initial and final parameter values are listed as an aluminum liner driven by the Atlas capacitor bank implodes an FRC. The table is the result of running the model described in this report for the Atlas set of parameters.

Parameter:	Initially:	At peak compression:
Liner Radius, R	5 cm	2.2 mm
Liner length, l	30 cm	30 cm
Liner thickness, d	1.1 mm	13 mm
Axial magnetic field, B_Z	5 T	2.7 kT
Plasma temperature, T	300 eV	2.4 keV
Plasma density, n	10^{23} m^{-3}	$5.4{\cdot}10^{25}$ m^{-3}
System resistance, R_l	1 mΩ	1 mΩ
Capacitance, C_C	0.3125 mF	0.3125 mF
Capacitor voltage, u_C	480 kV	96 kV
Total inductance, L_{tot}	39 nH	228 nH

Clearly, rather good results can be achieved. It is true that the only loss mechanism described in the model is the Bremsstrahlung radiation and no plasma-wall interaction is taken into account at all.

However, this is not the full story. The fractional burnup in this pulse is only just over 10^{-6}, and a plot of the radial time dependence reveals what is happening. At peak compression the pressure from the plasma and magnetic field is so large reversing the liner implosion into an explosion. This probably deforms the liner to such an extent making it lose contact with its electrodes.

It is thus only during a very short fraction of the total pulse when the conditions are such that they allow significant thermonuclear fusion. This is when the liner is confining the plasma through its inertia at the moment of motion reversion. The length of this time, the dwell time, is essential for the performance of the whole system.

In fig.C.5 are plotted the plasma temperature, the plasma number density, the fractional burnup and the axial magnetic field as functions of time for the Atlas implosion.

The difficulty in finding a set of parameters that substantially raise the fractional burnup is probably the main constraint for the whole MTF concept. A thicker liner has more inertia and may be able to confine the plasma for a longer time, but more inertia requires more power input for the same implosion velocities and compression ratio.

2.3.2 Action integral

The liner current heats the liner and depending on liner resistance and current intensity it will eventually melt or even vaporize. Since the implosion pulse is so short, no cooling of the liner is expected and the total resistive heat loss is deposited in the liner. In section 2.1.2 the action integral is defined as:

$$I_a = \int_t \frac{I(t)^2}{A_0^2} dt \tag{2.52}$$

As described in that section, at least part of the liner will be solid if the integral is below about $2{\cdot}10^{16}$ A^2s/m^4. If it is below about $4{\cdot}10^{16}$ A^2s/m^4, at least part of the liner will be liquid and if it exceeds about $5{\cdot}10^{16}$ A^2s/m^4, it will be totally melted and part of the liner will probably be vaporized. Figure C.6 shows the action integral for the Atlas implosion.

It is probably of crucial importance that the liner remains solid throughout the whole implosion, but not for sure. The important issue is that it is not deformed. If it is stable, melting may not be a problem although vaporization should most certainly be devastating. In this set of parameters at least part of the liner is obviously melted but a core of solid material should still contribute to the stabilization of the liner.

2.3.3 Energy budget

MTF is a two-stage process in which the stored electric energy first is transferred to the liner as it gains kinetic energy. In turn, this kinetic energy is transferred to the plasma as the liner compresses it. It was found that the first energy transfer has an efficiency of about 60%. The second transfer however, has an efficiency of just below 10%. The total efficiency is thus 6%. Figure C.7 shows the energy budget diagram.

Chapter 3

Parameter space for MTF

In order to understand how changing initial parameters effects the behaviour of the system, a MATLAB code was written that ran the original model for different sets of parameter values. The result was a survey of the parameter space for the MTF system.

3.1 An extended model

The new computer code runs the model of the MTF system a number of times, each time with a different choice of initial parameter values. Parameters that can be altered are:

Initial liner radius, R_0
Liner length, l
Initial magnetic field, B_0
Initial plasma temperature, T_0
Initial liner thickness, d_0
Initial plasma density, n_0
Return current path radius to liner radius ratio, a
System resistance, R_l
Capacitance, C_C
Initial capacitor voltage, u_0

The quantity according to which the system should be optimized is the Q-value. Therefore the initially stored energy is kept constant as well as the total plasma mass, as the maximum Q-value (represented by total burnup) also is kept constant. If the total plasma mass is M, and the liner length to initial liner radius ratio is constant and set to $l/R_0 = 6$, the initial liner radius is given by:

$$R_0 = \left(\frac{M}{3\pi(m_D + m_T)n_0} \right)^{1/3} \tag{3.1}$$

where m_D and m_T are the deuterium and tritium masses respectively.

As thermal conduction is not treated, the initial axial magnetic field B_0 is constant within the survey. The initial magnetic field is, in this case, chosen to be $B_0 = 5\text{T}$, as it is thought that this value is sufficient to prevent a major part of the negative effects from thermal conduction. Initial temperature T_0, initial plasma density n_0 and initial liner thickness d_0 are however parameters that could be altered in trying to achieve good performance.

In this survey, the temperature is kept constant as the number density is altered from 10^{20} m^{-3} to 10^{24} m^{-3} in four steps per change of factor 10 (i.e. $n_0 = (1,3,5,7,10,30,\ldots,10^4)(10^{20}\text{ m}^{-3})$. The liner thickness is altered from 0.1 mm to 10 mm in four steps per change of factor 10 (i.e. $d_0 = (0.1,0.3,0.5,0.7,1,\ldots,10)$ mm).

3.2 Survey of the parameter space

The code was run for the Atlas set of parameters:

$M = 1$ mg
$T_0 = 300$ eV
$C_C = 0.3125$ mF
$u_0 = 480$ kV

The driver parameters suggest the initially stored electric energy to be 36 MJ and the total fuel mass suggests the maximum fusion energy gain to be 338 MJ. The maximum theoretical Q-value hence is $Q = 9.4$. In fig. C.8 the Q-values for different initial values on plasma density and liner thickness are presented.

In the plot, it is clear that higher initial plasma density is preferable. However, the maximum plasma density of 10^{24} m^{-3} may not be possible to achieve in reality, or would at least be very difficult.

The results of the parameter space survey are not very promising. It seems like higher number density of the preformed FRC is the only way to go to improve the performance of the system.

Chapter 4

Conclusions

Magnetized Target Fusion offers an alternative way to achieve thermonuclear conditions in a fusion plasma, and this to a much lower cost than traditionally examined concepts. Thermonuclear conditions can be achieved in already existing facilities. This is possible because MTF does not need large superconducting coils (as magnetic fusion energy concepts usually do) and its energy density is high enough to allow the plasma volume to be rather small. Benefits over inertial confinement fusion originates from the introduction of a magnetic field which decreases the thermal conduction losses and also isolates the target from intrusion of impurities from the wall.

However, because of the short liner dwell time and thus short burn time, the fractional burnup hardly manage to exceed one percent. This is critical for the concept and if it is to become a reasonable alternative the dwell time must be extended to raise the burnup fraction.

The limitations of the MTF concept are completely different from those restricting the development of conventional concepts. Traditionally, plasma instabilities have been causing trouble. The FRC should, however, be stable during transformation and compression according to research done in the last decades, and liner implosions are stable too. Hence none of the most common constraints to fusion concepts are relevant to MTF.

To a certain extent, the development of an MTF reactor calls for different technical solutions than other fusion concepts and therefore one may still be optimistic about this approach.

Chapter 5

Reactor concepts

Although the prospects for magnetized target fusion are heavily reduced due to its constraints, the technical difficulties are of a completely different kind than those limiting "conventional" fusion concepts as the Tokamak and inertial confinement fusion. This fact gives indeed hope since constraints traditionally associated with fusion are not relevant to MTF. Undoubtedly fusion conditions can be achieved with an imploding liner on an FRC plasma. The problem is to sustain these conditions.

Apparently, there are two different ways for an MTF reactor to prove economical: it can either recover some (a lot) of the invested energy, or it can confine the compressed plasma by forces neutralizing the plasma and magnetic field pressure. In this chapter one example of how this can be done is presented of each of these variants and the economics of a fusion reactor built on these concepts is also discussed. Lastly some unusual applications are presented that would probably fit the MTF reactor.

5.1 Energy recovery

Electric energy inserted to the circuit from the capacitor bank could be recovered and used to recharge the capacitors during the second quarter current cycle if the liner is not destroyed. The liner runs the risk to be destroyed by either the current (which heats the liner due to its resistance), the plasma (which interacts with the liner wall) or fast neutrons (if the neutron yield is significant, which it of course would be in a fusion reactor). It can also be deformed by asymmetry in the implosion or by Rayleigh-Taylor instabilities and thus lose contact with the electrodes. Only if all these obstacles are small enough, energy recovery is possible.

As the liner contracts, the inductance of the circuit is altered since

$$L_{tot} = \frac{\mu_0 l}{2\pi} \cdot ln\frac{a}{R} + \frac{\mu_0 l}{8\pi} \tag{5.1}$$

At peak compression the total inductance is at its highest level and when the liner retracts towards its final shape it decreases. A parameter configuration where significant energy recovery is possible was investigated and the reactor concept is described below.

In this fusion reactor, the total resistance of the circuit is set to be $R_{tot} = 0.1$ mΩ. This is low, but a low resistance is imperative if the energy recovery is to be high enough. The resistance is a parameter of the construction and may be possible to keep low depending on the design of the current lines.

Initial radius of the liner is 13.5 cm and the length of the liner is 81 cm. A conical theta pinch forms, preheats and translates the FRC into the imploding liner. The formation and translation system has an efficiency of about 10%. This means that each pulse requires 18 MJ for plasma formation and translation resulting in a plasma with total plasma energy of 1.8 MJ. The preheated plasma has a temperature of 300 eV and a number density of $1.2{\cdot}10^{23}$ m^{-3}. Some of the formation energy should be possible to recover, maybe as much as 90%.

The repetition rate is 4 Hz. It is the insertion of new hardware material (new liners) that restricts the repetition rate. If the liner is solid throughout the whole implosion, it must both be taken out and a new one must be placed in position before the next pulse. However, the liner could as well crash into a wall of liquid aluminum (liner material) at the end of the pulse eliminating the problems of removing the used liner. The liner may even be liquid throughout the implosion, rotating to eliminate Rayleigh-Taylor instabilities. It would then reform against a rotating wall after each pulse. In that case one and the same liner is used over and over again, which could probably rise the repetition rate substantially.

Assuming the liner neither to be destroyed nor to loose contact with the electrodes, the energy recovery in this analysis is as large as 93.7%. Fig C.9 shows the energy budget of this fusion reactor configuration.

The total fusion energy produced in one pulse is 142 MJ and the initially stored electric energy in the capacitors is 710 MJ. If no energy recovery was done, the Q-value would have been $Q = 0.200$. However, 93.7% of the electric energy is recovered and the Q-value thus is $Q = 3.256$. In figure C.10 a flowchart is shown describing the energy economics per pulse.

Three major energy acquisition systems are used. A direct energy converter decelerates charged particles (alpha particles and unburned fusion fuels). This has an efficiency of about 65%. Most energy is acquired by the energy recovery, which recharges the capacitors almost completely (a fraction of the electric energy produced is recycled to the capacitors). Fast neutrons penetrate the liner and leave their energy in the blanket, which consists of liquid FLIBE salt (Fluor-LIthium-BEryllium), which is going through a thermal conversion system leaving its extra thermal energy in a heat exchanger. All energy losses are eventually gathered by this thermal conversion system which has an efficiency of 45%.

Four pulses each second results in an output (electric) effect of 160 MW. The construction cost of such a power plant is estimated to $200 million, where the capacitor bank for the liner implosion represents the major part. This number is in fact based on the cost for the Atlas facility, which was $50 million. Atlas's capacitor bank has an initial voltage of 480 kV and a capacitance of 0.3 mF. To drive the liner implosion in the power plant described here, a capacitor bank with an initial voltage of over 1 MV and a capacitance of 1.3 mF is assumed. This represents in fact 20 times the stored energy of Atlas, but only 4 times the capacitance and twice the voltage.

In appendix B the cost of electricity for the Energy Recovery MTF Power Plant Configuration is estimated to $0.04 per kWh.

5.2 Inertial confinement

The main difficulty in making the MTF concept economical is to increase the fractional burnup to over one or a few percent. If recovery of the capacitor energy is not possible, this burnup fraction must imperatively be risen quite a lot. It is the very short dwell time of the liner that sets these constraints. When the plasma and axial magnetic field are compressed by the liner, their pressure becomes so large that the liner immediately starts to expand resulting in a dwell time (and burn time) of no more than a couple of 100 ns. This is obviously not enough for a large fraction of the plasma to burn although thermonuclear conditions undoubtedly are obtained. If these conditions could be maintained for just a little longer (a few μs) a considerable fraction of the plasma would burn and there would indeed be hope to design a reactor that works.

One way to increase the dwell time would be to increase the liner weight and thus its inertia, either by changing liner material to one with higher density or to increase the liner thickness. It would then respond slower to the inner pressure trying to expand it but it would also require a stronger force to implode it and therefore a larger current (which means more stored electric energy and larger capacitor banks). Hence the cost to implode a heavier liner would rapidly eat the benefits. Also, the choice of liner material must concern many other things, such as plasma-wall interaction and resistivity. Chapter 3 shows that a larger thickness certainly increases the performance but not that much.

Accordingly, the liner should be light during compression and heavy at peak compression and afterwards. One idea could be the double-liner: two liners are used, one liner for compression and one for keeping the thermonuclear conditions once achieved. For example, the thin aluminum liner used to compress the plasma could be supported after peak compression by an incompressible liquid (maybe water). The liquid is let into the expanding volume outside the liner through valves that close at peak compression, pre-

venting the liner to retract. This system requires the liquid to be inserted at a pressure of megabars, which is not too difficult to achieve. The main difficulty is probably the demands on the vessel containing the compressed plasma and liner and the surrounding incompressible material. It must be constructed to withstand rather strong tension.

The incompressible liquid may enable the dwell time to be several μs. In that case, the fractional burnup is expected to exceed 10% and would maybe even approach total burnup.

5.3 Other applications

Besides the obvious area of use for an MTF power plant to produce electricity to the grid, several other applications could come in question. The advantages of MTF include that the reactor possibly can be quite compact, and that the plasma configuration has open field lines, which enables direct conversion to electricity and thus a higher efficiency. Both these advantages are strengthened if exotic fuels such as deuterium-helium-3 are used. No bulky and heavy blanket is needed and almost all energy can be converted to electricity by direct conversion.

One application that would probably fit MTF is the use as portable power plant for instance on ships. Today small nuclear reactors are used to provide ships with energy, and this is an area that MTF could be used within, probably in contrast to many other fusion concepts.

MTF could very well be used as a space propulsion system. Again the use of exotic fuels would be preferable since the elimination of a blanket lowers the weight of the engine. Also, if all reaction products are charged particles, the plasma ashes from each pulse could be guided out through a magnetic nozzle to provide thrust. This application has certainly the potential of revolutionizing space flight, shortening distances and travelling times in space.

Aknowledgments

The author wishes to express his gratitude to Dr. J. Scheffel for the supervision of this master thesis project, and also to Dr. R.E. Siemon and Dr. I.R. Lindemuth at the Los Alamos National Laboratory, with whom valuable email correspondance was made.

Bibliography

[1] R.E. Siemon, I.R. Lindemuth, K.F. Shoenberg: *Why Magnetized Target Fusion Offers A Low-Cost Development Path for Fusion Energy*, Los Alamos National Laboratory, LA-UR-97-4747 (1997)

[2] R.E. Siemon, et al.: *Measurements of Solid Liner Implosion for Magnetized Target Fusion*, Los Alamos National Laboratory, LA-UR-00-4496 (2000)

[3] A.E. Robson: *The Dense Z-pinch as a Small Fusion Reactor*, second international conference on dense z-pinches, Laguna Beach, (1989)

[4] A.E. Robson: *Evolution of a Z-pinch With Constant dI/dt*, Nuclear Fusion, Vol. 28, No. 12, (1988)

[5] J. Scheffel, P. Brunsell: *Fusionsplasmafysik - introduktion till fysiken bakom fusionsenergi*, Alfvn Laboratory, Royal Institute of Technology, Stockholm (2000)

[6] K.F. Schoenberg, R.E. Siemon: *Magnetized Target Fusion - A Proof-of-Principle Research Proposal*, Los Alamos National Laboratory, LA-UR-98-2413 (1998)

[7] D.D. Ryutov, R.E. Siemon: *Magnetized Plasma Configurations for Fast Liner Implosions: A Variety of Possibilities*, Los Alamos National Laboratory, LA-UR-99-3628 (1999)

[8] R.E. Siemon, et al.: *The Relevance of Magnetized Target Fusion (MTF) to Practical Energy Production*, Los Alamos National Laboratory, LA-UR-99-2956 (1999)

[9] G.A. Wurden, et al.: *Magnetized Target Fusion: A burning FRC plasma in an imploded metal can*, Los Alamos National Laboratory, LA-UR-98-5674 (1998)

[10] H.-S. Bosch, G.M. Hale: *Improved Formulas for Fusion Cross-sections and Thermal Reactivities*, Nuclear Fusion, Vol. 32, No. 4, (1992)

[11] I.R. Lindemuth, R.C. Kirkpatrick: *Parameter Space for Magnetized Fuel Targets in Inertial Confinement Fusion*, Nuclear Fusion, Vol. 23, No. 3, (1983)

[12] M. Tuszewski: *Field Reversed Configurations*, Nuclear Fusion, Vol. 28, No. 11, (1988)

[13] H. Momota, et al.: *Characteristics of D-3He Fueled FRC Reactor: ARTEMIS-L*, National Institute for Fusion Science, Nagoya, Japan, (1993)

[14] W.M. Parsons, et al.: *The ATLAS Project*, Los Alamos National Laboratory, LA-UR-96-3440 (1996)

[15] H.U. Rahman, F.J. Wessel, N. Rostoker: *Staged Z Pinch*, Physical Review Letters, Vol. 74, No. 5, (1995)

[16] P. Ney, H.U. Rahman, N. Rostoker, F.J. Wessel: *UCI Staged Z Pinch*, CP409. Dense Z Pinches: Fourth International Conference, (1997)

[17] L.J. Perkins, et al.: *High Density, High Magnetic Field Concepts for Compact Fusion Reactors*, Sixteenth IAEA Fusion Energy Conference, IAEA-CN-64/GP-18 (1996)

Appendix A

Reactivity model

The reactivity $\langle \sigma v \rangle_{DT}$ used in this report is the reactivity described by H.S. Bosch and G. M. Hale [10]. It is defined as:

$$\langle \sigma v \rangle = C_1 \cdot \theta \sqrt{\xi / (m_r c^2 T^3)} e^{-3\xi} \tag{A.1}$$

where

$$\theta = T / \left(1 - \frac{T(C_2 + T(C_4 + TC_6))}{1 + T(C_3 + T(C_5 + TC_7))} \right) \tag{A.2}$$

$$\xi = \left(B_G^2 / (4\theta) \right)^{1/3} \tag{A.3}$$

If T is the ion temperature given in keV, the reactivity $\langle \sigma v \rangle_{DT}$ is in cm^3/s. For DT fusion the parameters are given as:

Parameter:	For the reaction D(T,n)4He:
$B_G \left(\sqrt{keV} \right)$	34.3827
$m_r c^2 \, (keV)$	1 124 656
C_1	$1.17302 \cdot 10^{-9}$
C_2	$1.51361 \cdot 10^{-2}$
C_3	$7.51886 \cdot 10^{-2}$
C_4	$4.60643 \cdot 10^{-3}$
C_5	$1.35000 \cdot 10^{-2}$
C_6	$-1.06750 \cdot 10^{-4}$
C_7	$1.36600 \cdot 10^{-5}$

For 0.2 keV ¡ T_i ¡ 100 keV the reactivity maximal deviation is 0.25%.
In figure C.11 the reactivity is plotted.

Appendix B

Characteristics of the Energy Recovery MTF Power Plant Configuration

Below are presented assumptions on which a rough estimate of the cost of electricity from the Energy Recovery MTF Power Plant Configuration would be. The assumption of the direct cost of the power plant is based upon the cost of the Atlas facility, which was $50 million. The power plant capacitor bank is assumed to contribute to the largest fraction of the cost of the power plant. It should be able to store 20 times the energy stored within the Atlas capacitor bank. However, the cost of the facility should not be proportional to the energy stored. Once the technique of building large capacitor banks is developed it should be possible to mass-produce it and construct rather large devices to a limited cost.

Electricity production:	160 MW
Annual electricity production (P):	109 kWh
Total direct cost:	M$ 200
Total capital cost:	M$ 360
Annual cost (C_A):	M$ 30
Annual operational cost (C_{op}):	M$ 10
COE [$= (C_A + C_{op})/P$]:	$ 0.04 / kWh

It is here assumed that the plant in average operates at 75% of full capacity, and the lifetime is expected to be some 30 years. This evaluation of the cost of electricity is inspired by the evaluation of the ARTEMIS-L cost of electricity [13].

Appendix C

Plots and figures

In this chapter plots and figures referred to in the previous chapters are presented.

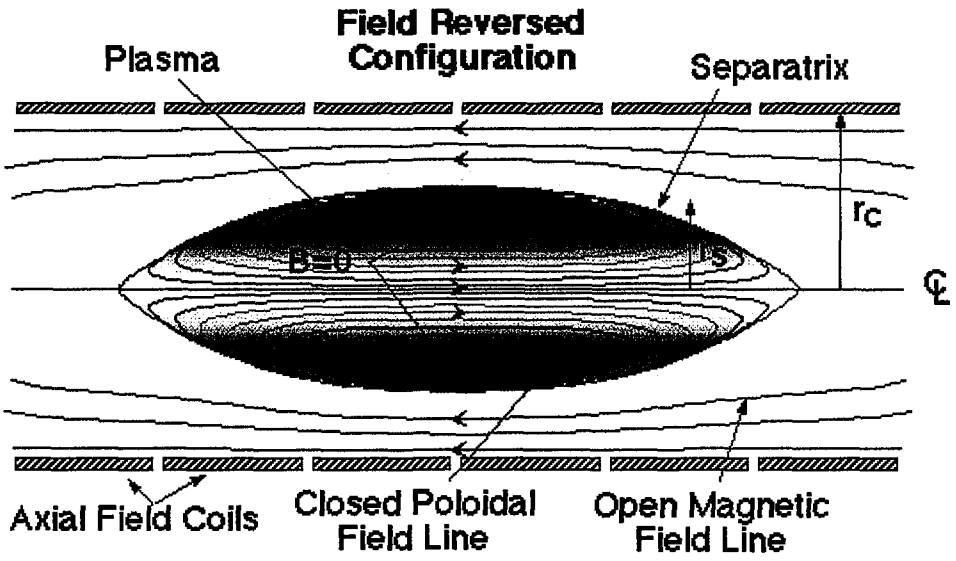

Figure C.1: Schematic figure of the Field Reversed Configuration (FRC). Indicated in the figure is the separatrix that separates the open magnetic field from the closed poloidal magnetic field. Further, r_s is the radius of the separatrix, and r_c is the radius of the axial field coils.

http://www.aa.washington.edu/AERP/RPPL/frc_intro.html

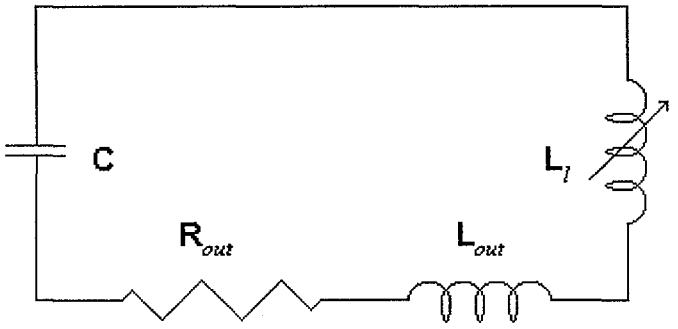

Figure C.2: Circuit plan for the liner, the capacitor bank and the current feed system.

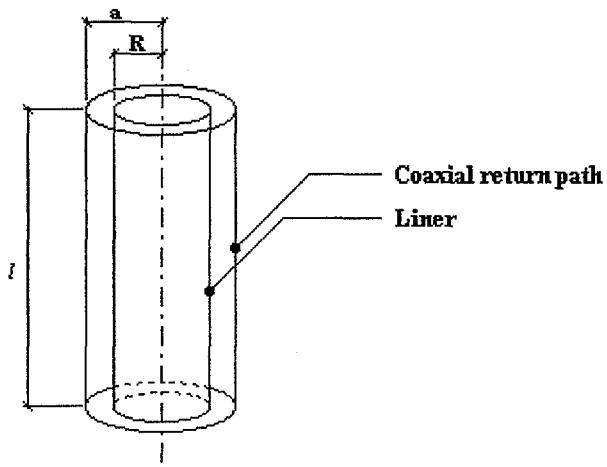

Figure C.3: The current return-path is coaxial to the liner.

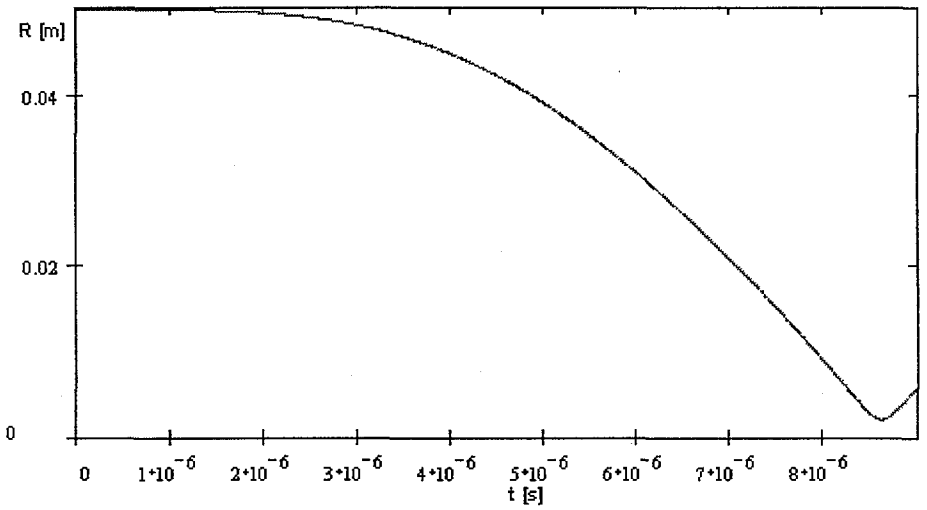

Figure C.4: Radius as a function of time for a liner imploded by the Atlas capacitor bank.

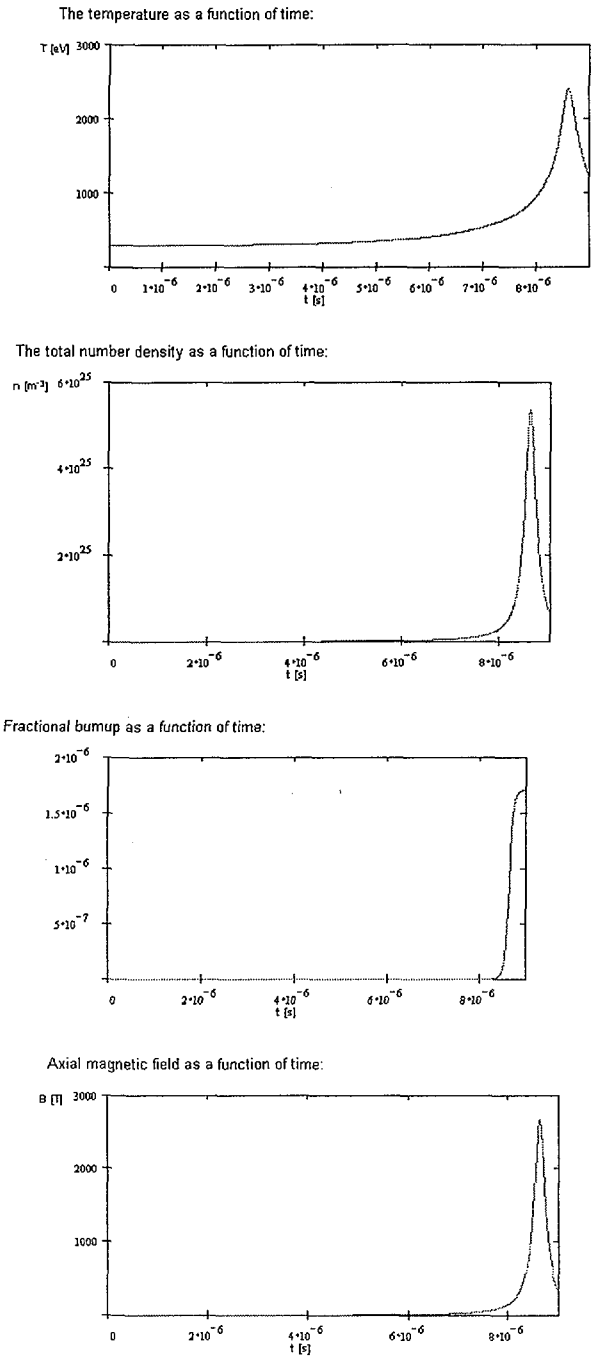

Figure C.5: Some essential quantities as functions of time.

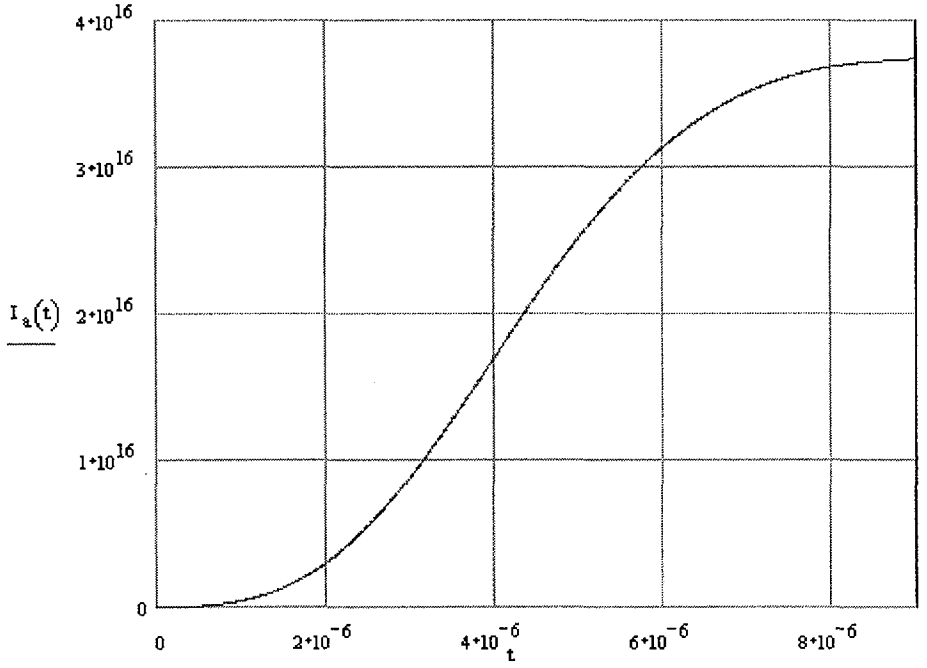

Figure C.6: The action integral as a function of time for the Atlas implosion.

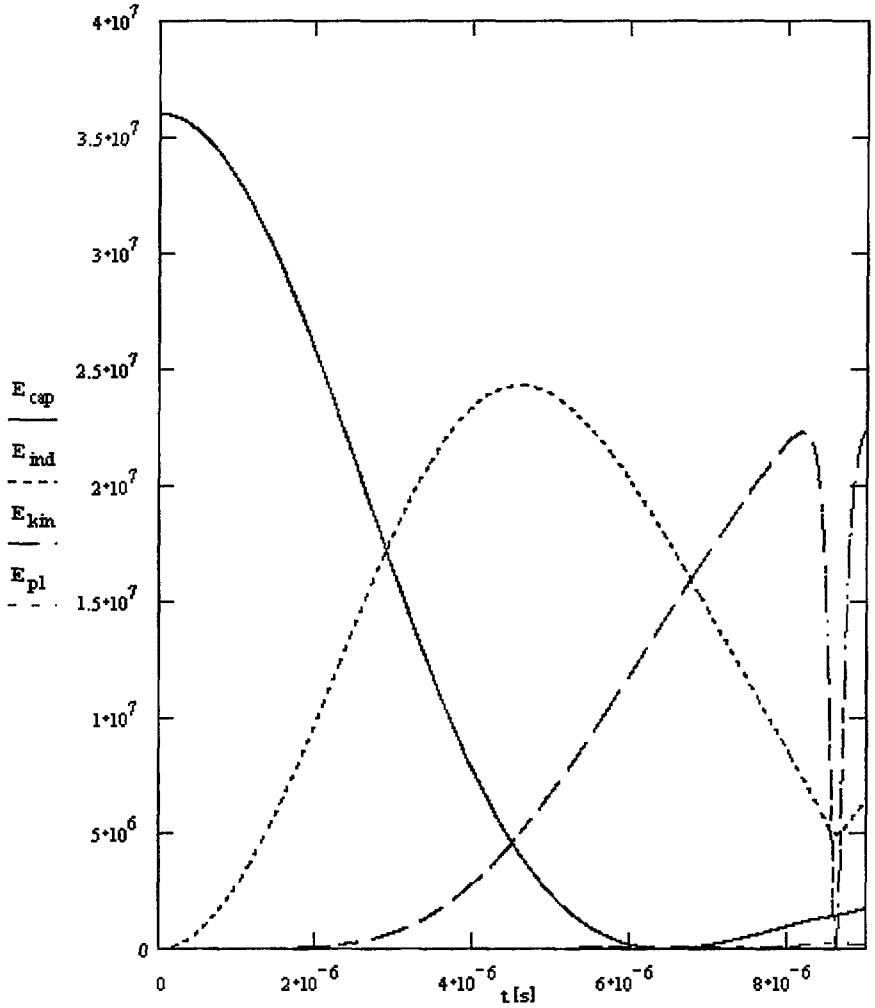

Figure C.7: Energy budget of the Atlas implosion. E_{cap} is the electric energy stored in the capacitors, E_{ind} is the magnetic energy stored in the inductor, E_{kin} is the kinetic energy of the liner and E_{pl} is the kinetic energy of the plasma. Note that the kinetic energy of the liner drops as the liner reverses at peak compression.

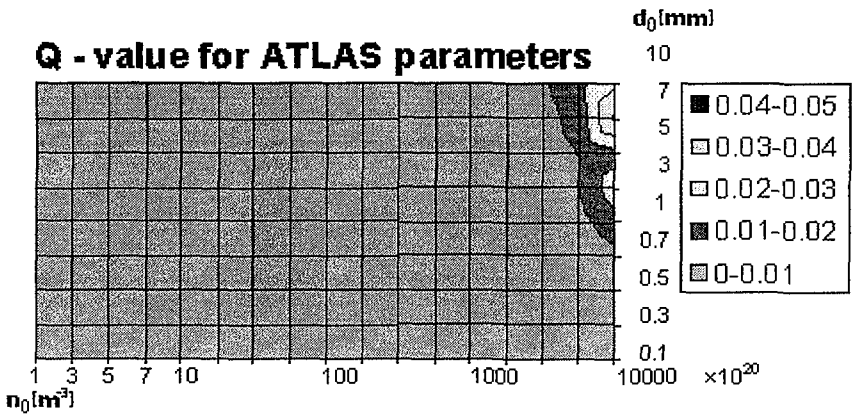

Figure C.8: Parameter space for Atlas parameters.

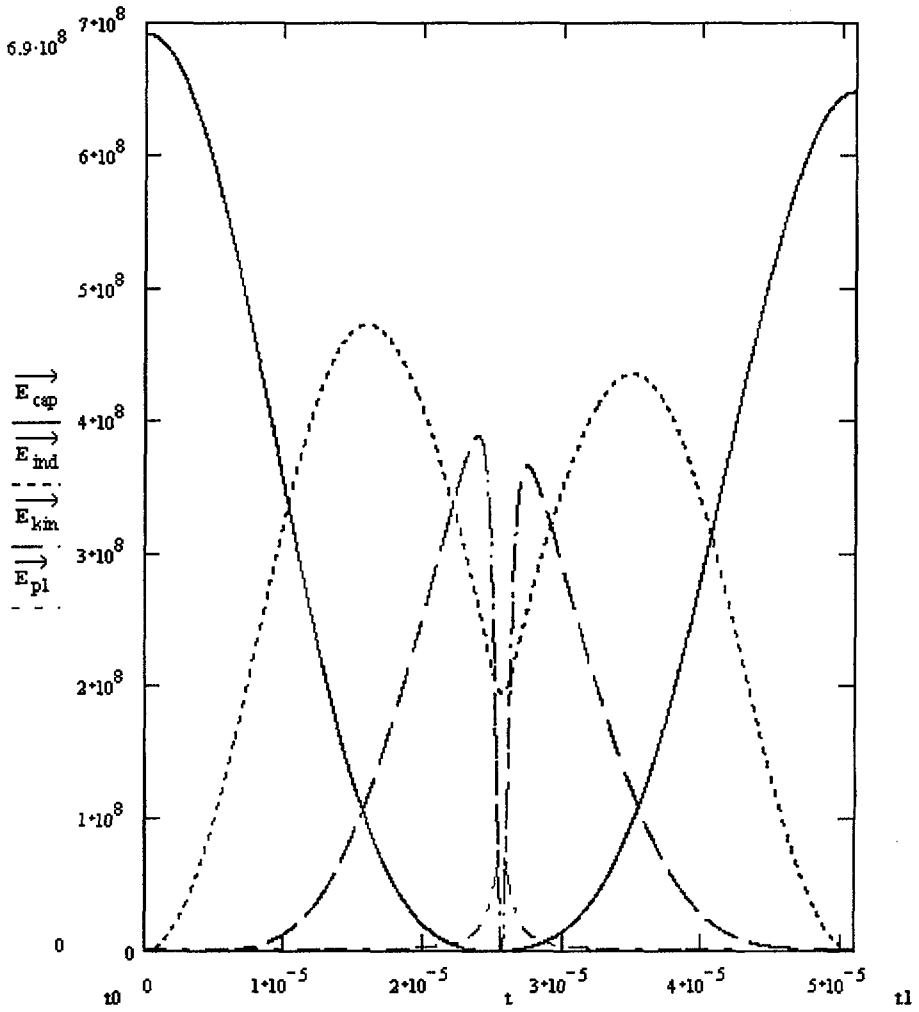

Figure C.9: Energy budget of the Energy Recovery MTF Power Plant Configuration. There is a significant recovery of capacitor energy (93.7%). E_{cap} is the capacitor energy, E_{ind} is the inductor energy, E_{kin} is the kinetic energy of the liner and E_{pl} is the plasma kinetic energy.

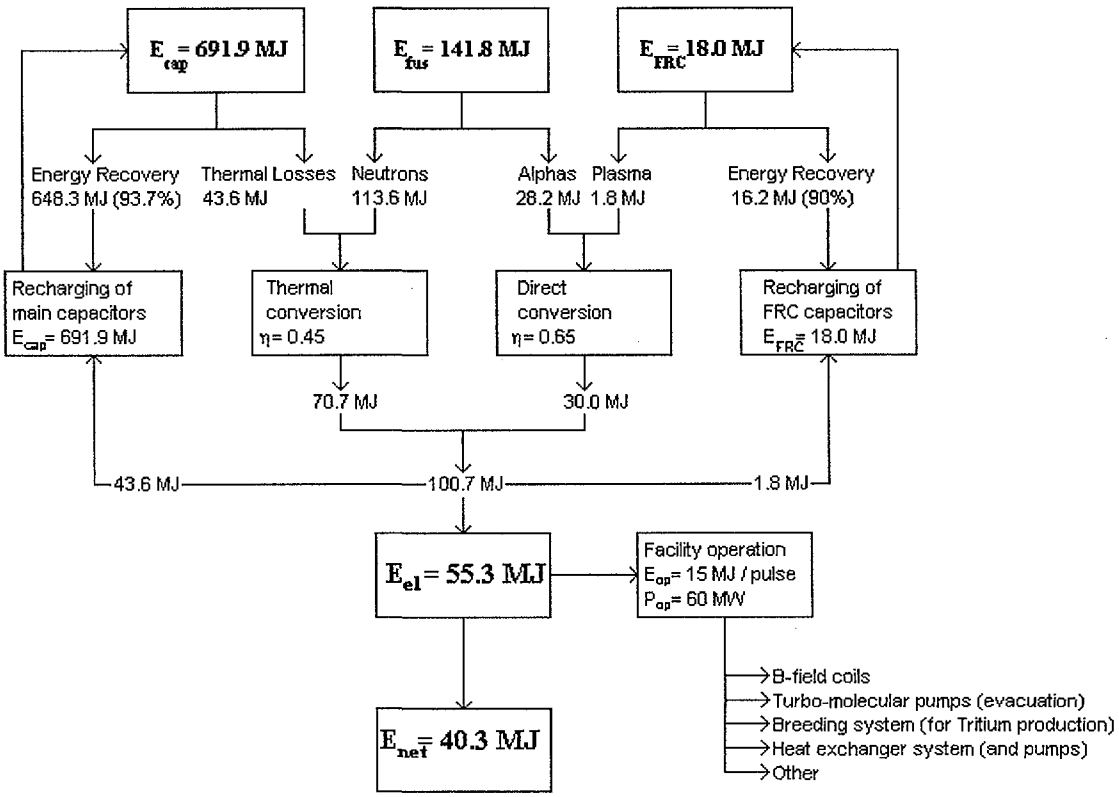

Figure C.10: Energy flowchart for the Energy Recovery MTF Power Plant Configuration.

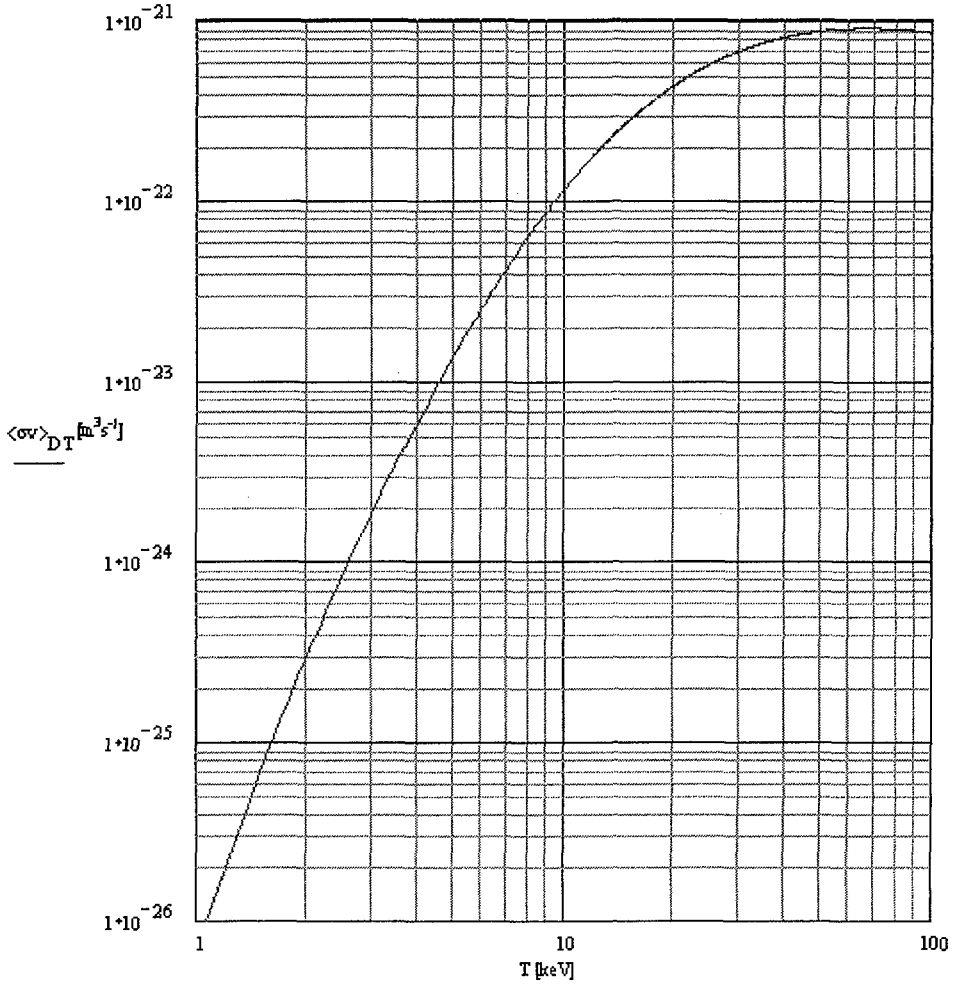

Figure C.11: Reactivity $\langle \sigma v \rangle_{DT}$ as a function of ion temperature, according to H.S. Bosch and G. M. Hale [10].

CIC-1300-0126 (11-99)

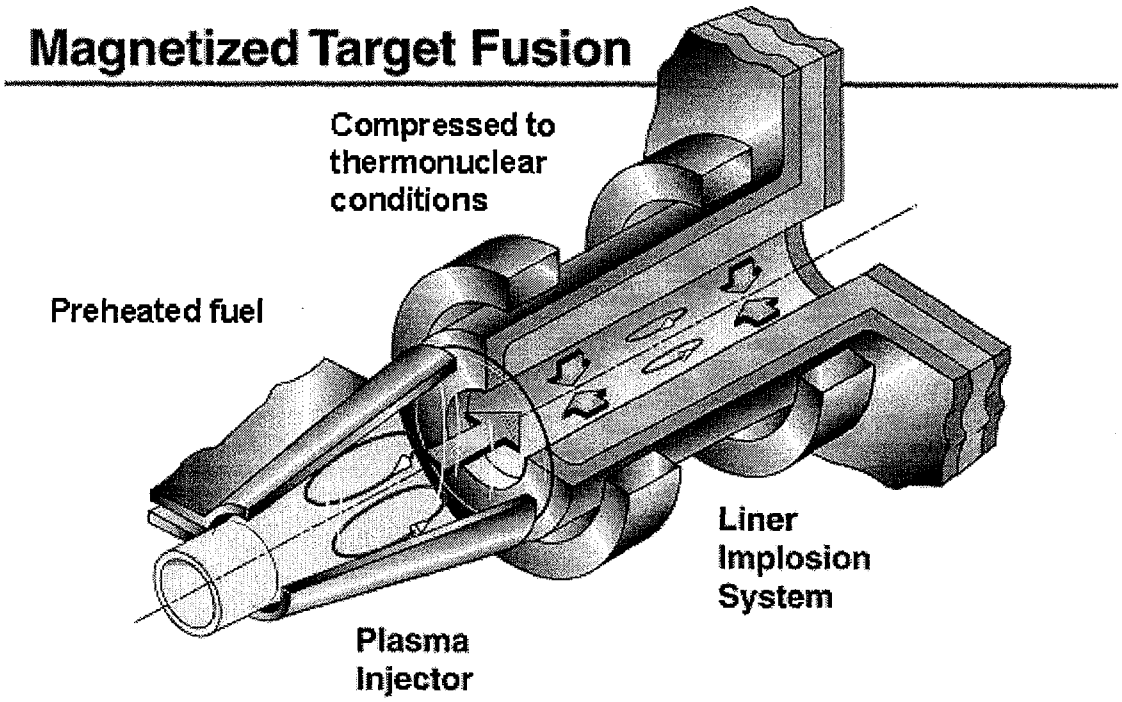

Figure C.12: Schematic figure of the MTF system, including the conical theta pinch (left) and the implosion chamber (right).

http://fusionenergy.lanl.gov/mtf.htm#MTF

Abstract

Magnetized Target Fusion (MTF) is a possible pathway to thermonuclear fusion different from both magnetic fusion and inertial confinement fusion. An imploding cylindrical metal liner compresses a preheated and magnetized plasma configuration until thermonuclear conditions are achieved.

In this report the Magnetized Target Fusion concept is evaluated and a zero-dimensional computer model of the plasma, liner and circuit as a connected system is designed. The results of running this code are that thermonuclear conditions are achieved indeed, but only during a very short time.

At peak compression the pressure from the compressed plasma and magnetic field is so large reversing the liner implosion into an explosion. The time period of liner motion reversal is termed the dwell time and is crucial to the performance of the fusion system. Parameters as liner thickness and plasma density are certainly of significant importance to the dwell time, but it seems like a reactor based on the MTF principle hardly can become economic if not innovative solutions are introduced. In the report two such solutions are presented as well.

Keywords : magnetized target fusion, MTF, zero-dimensional model, field reversed configuration, FRC